1758–1764 *Nucleic Acids Research, 1996, Vol. 24, No. 9*

Binding of DNA oligonucleotides to sequences in the promoter of the human *bcl-2* gene

Wendy M. Olivas[+] and L. James Maher, III[1,*]

Eppley Institute for Research in Cancer and Allied Diseases and the Department of Biochemistry and Molecular Biology, University of Nebraska Medical Center, 600 S. 42nd Street, Omaha, NE 68198-6805, USA and [1]Department of Biochemistry and Molecular Biology, Mayo Foundation, 200 First Street, SW, Rochester, MN 55905, USA

Received November 27, 1995; Revised and Accepted March 14, 1996

ABSTRACT

Duplex DNA recognition by oligonucleotide-directed triple helix formation is being explored as a highly specific approach to artificial gene repression. We have identified two potential triplex target sequences in the promoter of the human *bcl-2* gene, whose product inhibits apoptosis. Oligonucleotides designed to bind these target sequences were tested for their binding affinities and specificities under pseudo-physiological conditions. Electrophoretic mobility shift and dimethyl sulfate footprinting assays demonstrated that an oligonucleotide designed for simultaneous recognition of homopurine domains on alternate duplex DNA strands had the highest affinity of any oligonucleotide tested. Modifications to render this oligonucleotide nuclease-resistant did not reduce its binding affinity or specificity. In additional studies under various pH conditions, pyrimidine motif complexes at these target sequences were found to be stable at pH 8.0, despite the presumed requirement for protonation of oligonucleotide cytidines. In contrast, purine motif complexes, typically considered to be pH independent, were highly destabilized at decreasing pH values. These results indicate that a natural sequence in the human *bcl-2* promoter can form a stable triplex with a synthetic oligonucleotide under pseudo-physiological conditions, and suggest that triple helix formation might provide an approach to the artificial repression of *bcl-2* transcription.

INTRODUCTION

Oligonucleotide-directed triple helix formation is a highly specific strategy for designing potential artificial gene repressors (1–5). *In vitro* experiments provide evidence that triplexes can block DNA binding proteins (6–8) and inhibit transcription initiation (2,9–13). Recognition of homopurine/homopyrimidine sequences involves hydrogen bonds between oligonucleotide bases and purine bases in the major groove of duplex DNA. Triple helix formation occurs in either of two distinct patterns, termed the pyrimidine (Pyr) motif and purine (Pur) motif (4). In the pyrimidine motif, oligonucleotides bind parallel to the purine strand of the duplex by Hoogsteen hydrogen bonding to form T·A·T and C+·G·C base triplets (1). In the purine motif, oligonucleotides bind antiparallel to the purine strand of the duplex by reverse Hoogsteen hydrogen bonding to form A·A·T (or T·A·T) and G·G·C base triplets (4). We are interested in the possibility that triple helix formation might be used to artificially regulate the expression of disease-related genes.

The product of the *bcl-2* proto-oncogene acts as a negative regulator of programmed cell death (apoptosis; 15–17). Apoptosis not only provides a termination option for cells that are dangerously damaged, but also plays a key role in normal T and B cell development (18–20). In some tissues, the propensity toward apoptosis appears to be regulated by the ratio of *bcl-2* and *bax* proteins. Increases in *bax* concentrations counter the apoptotic suppression by *bcl-2* (21). One of the most common cytogenetic abnormalities in non-Hodgkin B cell lymphomas is the translocation t(14;18)(q32;q21). This translocation places the *bcl-2* gene at 14q21 under the control of the immunoglobulin heavy-chain gene enhancer, resulting in *bcl-2* overexpression (22,23). Studies of transgenic mice overexpressing *bcl-2* show an increase in both B and T cell survival, leading to lymphomas derived from both cell types (22). In contrast, *bcl-2* –/– knockout mice undergo profound apoptotic deletion of B and T cells shortly after birth (24).

Therapeutic techniques such as radiation and many chemical agents act by inducing apoptosis. This observation suggests that approaches to reducing the damage threshold required for induction of cell death by an apoptotic signal may sensitize tumor cells to chemotherapeutic agents. One such approach might be to artificially reduce *bcl-2* levels in cells by repression of *bcl-2* transcription via triple helix formation targeted to the *bcl-2* promoter region. The human *bcl-2* gene is transcribed from two promoters (P1 and P2; Fig. 1). The major promoter (P1) lacks a TATA box, is GC rich, contains seven consensus Sp1 binding sites, and displays multiple transcription initiation sites (23). We have identified two homopurine sequences just upstream of this major *bcl-2* promoter that might serve as triplex target sites.

We wished to design oligonucleotides that might bind the *bcl-2* target sequences with high specificity and affinity under physiological conditions. Electrophoretic mobility shift titrations were performed to estimate oligonucleotide affinities, while dimethyl sulfate footprinting assays were used to analyze oligonucleotide recognition and induced changes in the structure of the duplex

* To whom correspondence should be addressed

[+]Present address: Department of Molecular and Cellular Biology, University of Arizona, Tucson, AZ 85721, USA

target upon triplex formation. We report that under pseudo-physiological conditions, an oligonucleotide designed for adjacent purine and pyrimidine motif recognition binds homopurine domains on alternate duplex DNA strands with high affinity. This result provides an example of a naturally-occurring target sequence for which alternate strand triple helix formation clearly increases binding affinity relative to recognition of a single homopurine domain. Modifications to render this high-affinity oligonucleotide nuclease-resistant did not reduce its binding affinity. While many pyrimidine motif oligonucleotides require an acidic pH to protonate cytidine residues for tight binding to duplex DNA, the pyrimidine motif complexes in this study were remarkably stable at pH 8.0. In contrast, the stabilities of purine motif complexes, often considered to be pH independent, were in this study highly reduced at decreasing pH values. Together, these results identify oligonucleotides that bind tightly to the human *bcl-2* promoter under pseudo-physiological conditions. These results suggest a possible strategy for artificial repression of *bcl-2* transcription.

MATERIALS AND METHODS

Oligonucleotides

Oligonucleotide sequences are shown in Figure 1B. Oligonucleotides were synthesized by phosphoramidite chemistry on an ABI Model 380B DNA synthesizer, purified by denaturing polyacrylamide gel electrophoresis, eluted from gel slices, and desalted by Sep-Pak C_{18} cartridge chromatography (Waters). Oligonucleotides were quantitated by absorbance at 260 nm using molar extinction coefficients (M^{-1} cm^{-1}) of 15 400 (dA), 11 700 (dG), 7300 (dC), 5700 (dMe5C) and 8800 (dT), assuming no hypochromicity. Oligonucleotides comprising the target duplexes were annealed as follows: 500 pmol each of oligonucleotides **A** and **B** for the Pur1 duplex or oligonucleotides **C** and **D** for the Pur2 duplex were mixed with 2 µl 5 M NaCl and brought to a total volume of 42 µl with H_2O. This annealing reaction mixture was incubated at 75°C for 12 min and then gradually cooled to 25°C. Thirty pmol of the resulting oligonucleotide duplexes were radiolabeled using the Klenow fragment of DNA polymerase I and [α-^{32}P]dATP in the presence of 0.1 mM dGTP, dTTP and dCTP. The resulting labeled duplex oligonucleotides were purified by precipitation from ethanol in the presence of ammonium acetate, and resuspended in H_2O.

Electrophoretic DNA mobility shift assays

Four different binding buffers were employed in these studies: pH 5.0 (100 mM NaOAc, pH 5.0, 5 mM NaCl, 10 mM $MgCl_2$); pH 7.2 (100 mM MOPS, pH 7.2, 6 mM $MgCl_2$); pH 7.4 [also termed nuclear extract buffer, NEB; 20 mM Hepes, pH 7.4, 5 mM $MgCl_2$, 100 mM KCl, 10% (v/v) glycerol]; and pH 8.0 (25 mM Tris–HCl, pH 8.0, 6 mM $MgCl_2$). Binding reaction mixtures contained labeled duplex (50 000 c.p.m.; ~0.1 pmol), either 1 µl of 10× binding buffer or 2 µl of 5× binding buffer, 1 µl of 1 mg/ml yeast tRNA, 1 µl of oligonucleotide (to yield the indicated final concentration) and H_2O in a final volume of 10 µl. Reaction mixtures were incubated at 22°C for 5 h and were then supplemented with 1 µl of an 80% glycerol solution containing bromophenol blue. Reactions were analyzed by electrophoresis through 20% native polyacrylamide gels (19:1 acrylamide:bisacrylamide) prepared in electrophoresis buffer [for pH 5.0: 100 mM NaOAc, pH 5.0, 1 mM $MgCl_2$; for pH 7.2: 100 mM MOPS, pH 7.2, 6 mM $MgCl_2$; for pH 8.0 (used for both pH 7.4 and 8.0 binding buffers): 100 mM Tris base, 110 mM boric acid, 2 mM EDTA, 8 mM $MgCl_2$]. Electrophoresis was performed with recirculation at 4°C overnight (9 V/cm). The resulting gel was imaged and quantified by storage phosphor technology using a Molecular Dynamics PhosphorImager.

Analysis of DNA gel mobility shift titrations

The apparent fraction, θ of target duplex bound by oligonucleotide was calculated for each gel lane using the definition:

$$\theta = S_{triplex} / (S_{triplex} + S_{duplex}) \quad \mathbf{1}$$

where $S_{triplex}$ and S_{duplex} represent the storage phosphor signal for triplex and duplex complexes respectively. Values of the apparent triplex dissociation constant, K_d, were obtained by least squares fitting of the data to the binding isotherm:

$$\theta = ([O]^n / K_d^n) / (1 + [O]^n / K_d^n) \quad \mathbf{2}$$

where [O] is the concentration of oligonucleotide, and n is the Hill coefficient (25).

Dimethyl sulfate footprinting

Pur1 and Pur2 duplexes were each ligated into plasmid pG5E4T that had been cleaved by *Bam*HI and *Pst*I (11). Clones bearing the desired insertions were confirmed by sequencing. A 356 bp *Hin*dIII–*Sac*I restriction fragment from the Pur1-containing plasmid and a 361 bp *Hin*dIII–*Sac*I restriction fragment from the Pur2-containing plasmid were then prepared and dephosphorylated with calf intestinal alkaline phosphatase. The Pur1 and Pur2 fragments were uniquely end-labeled on strands **B** and **D** respectively, using polynucleotide kinase (see Fig. 1). For some experiments, the Pur2 fragment was uniquely end-labeled on strand **C** using the Klenow fragment of DNA polymerase I (see Fig. 1). Labeled fragment (50 000 c.p.m.; ~0.1 pmol) was incubated with either 1 µl of 10× pH 8.0 binding buffer or 2 µl of 5× nuclear extract buffer (NEB), 1 µl of 1 mg/ml yeast tRNA, 1 µl of 10 µM oligonucleotide, and H_2O in a final volume of 10 µl. Binding reactions were incubated overnight at 22°C. Dimethyl sulfate [1 µl of a 4% (v/v) aqueous solution] was added to each reaction mixture and allowed to incubate for 30 min at 4°C. Reactions were terminated with 5 µl of stop mix [1.5 M NaOAc, 7% (v/v) β-mercaptoethanol and 100 µg/ml yeast tRNA]. For formic acid treatment, 25 µl of formic acid was allowed to incubate with reaction mixture for 2 min at 22°C, then the reaction was terminated with 180 µl of HZ stop mix (0.3 M NaOAc, 0.1 mM EDTA, 25 µg/ml tRNA). Following ethanol precipitation, 100 µl of 10% piperidine was added, and the samples were incubated for 30 min at 90°C. Piperidine was removed by repeated lyophilization. The DNA was then resuspended in 5 µl of formamide dye mix, heated to 90°C, electrophoresed on an 8% polyacrylamide sequencing gel [19:1 (acrylamide:bisacrylamide)] containing 7.5 M urea in 0.5× TBE buffer (50 mM Tris base, 55 mM boric acid, 1 mM EDTA), and imaged by storage phosphor technology.

RESULTS

Experimental design

Studies of triple helix formation often employ non-physiological conditions such as acidic pH and/or low monovalent cation concentrations. We wished to study triple helix formation under physiological conditions at a natural target sequence. The *bcl-2* gene,

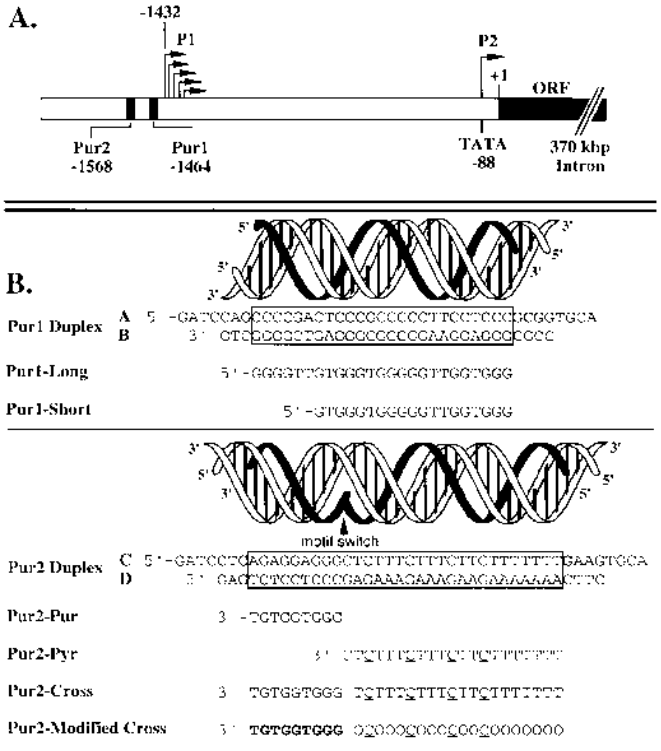

Figure 1. Experimental design. (**A**) Schematic illustration of *bcl-2* gene structure. Sites of the major TATA-less promoter (P1) and the minor promoter (P2) are indicated. Locations of the Pur1 and Pur2 homopurine target sequences are shown. (**B**) The Pur1 and Pur2 duplex DNA targets are formed by annealing complementary oligonucleotides **A** + **B** and **C** + **D** respectively. The Pur1 and Pur2 homopurine sequences from the *bcl-2* gene are boxed. Triplex oligonucleotides bind in the major groove of the target duplexes at the indicated positions. Graphical representations of triple-helical complexes are shown above sequences, with black ribbons denoting bound oligonucleotides. The diagrams depict intended molecular interactions. High resolution structural characterization of these complexes is not undertaken in this report. The motif switch for **Pur2-Cross** and **Pur2-Modified Cross** was executed by deletion of a cytidine residue at the junction. Underlined C residues represent 5-methylcytidine. Bold letters indicate a phosphorothioate backbone. O residues represent 2′-*O*-methylthymidine.

whose product inhibits apoptosis, contains two potential triplex target sequences just upstream of the predominant promoter, P1 (Fig. 1A; 26). One target sequence, termed Pur1, is located 32 bp upstream of the 5′-most major transcription start site (position –1432; Fig. 1A; 23) and consists of a 25 base purine-rich sequence with three pyrimidine interruptions (Fig. 1B). The second target sequence, termed Pur2, is located 136 bp upstream of the first major transcription start site and consists of two adjacent homopurine sequences; nine purines on one strand of the duplex directly adjacent to 21 purines on the opposite strand (Fig. 1B). To facilitate electrophoretic mobility analyses of oligonucleotide binding and to simplify cloning procedures, synthetic duplexes were designed containing the Pur1 and Pur2 sequences (Pur1 duplex and Pur2 duplex respectively; Fig. 1B).

The purine triple helix motif, most appropriate for guanine-rich target sites, was used to design triplex oligonucleotides to recognize the Pur1 target sequence. Oligonucleotide **Pur1-Long** was designed to span the entire Pur1 region, with thymidine residues used to cross interrupting pyrimidines in the target (Fig. 1B). **Pur1-Short**, which recognizes only 19 bases of the target, was designed to avoid two of the three interrupting pyrimidines of the target sequence (Fig. 1B).

It has previously been shown that oligonucleotides utilizing consecutive pyrimidine motif and purine motif sequences can simultaneously recognize purine domains on opposite strands of duplex DNA, such as those in the Pur2 target sequence (27–31). Target recognition is accomplished by switching triplex motifs, and thus relative strand polarities, as the oligonucleotide crosses between purine domains. The pyrimidine triple helix motif, appropriate for an adenine-rich target site, was used to design oligonucleotide **Pur2-Pyr** to recognize the 19 base domain of the Pur2 target sequence (Fig. 1B). **Pur2-Pur** was designed to recognize the nine base domain of the Pur2 target using the purine motif (Fig. 1B). These two oligonucleotides were then combined in the design of **Pur2-Cross** intended to simultaneously recognize both purine domains of the Pur2 target sequence (Fig. 1B). Using the strategy devised by Beal and Dervan (27), a cytidine residue was removed from the 5′-pyr motif:pur motif-3′ junction of **Pur2-Cross** to allow the oligonucleotide to more smoothly cross the major groove between the alternate strand homopurine regions. In addition, all cytidines in oligonucleotides for triple helix formation were modified to 5-methylcytidines to enhance binding at physiological pH (32). Electrophoretic mobility shift titrations allowed estimation of oligonucleotide binding affinities for *bcl-2* duplex targets, while dimethyl sulfate (DMS) footprinting assays were used to study details of oligonucleotide binding.

Table 1. Triplex K_d values[a]

ODN	pH	M^+	K_d (M)	Relative affinity[b]
Pur1-Long	5.0	–	$>>2.5 \times 10^{-6}$	<<0.02
	7.2	–	1.3×10^{-6}	0.05
	8.0	–	2.3×10^{-7}	0.27
Pur1-Short	5.0	–	$>>2.5 \times 10^{-6}$	<<0.02
	7.2	–	1.0×10^{-6}	0.06
	8.0	–	4.7×10^{-7}	0.13
Pur2-Pur	5.0	–	$>>2.5 \times 10^{-6}$	<<0.02
	7.2	–	$>>2.5 \times 10^{-6}$	<<0.02
	8.0	–	$>>2.5 \times 10^{-6}$	<<0.02
Pur2-Pyr	5.0	–	4.4×10^{-8}	1.4
	7.2	–	1.1×10^{-7}	0.55
	7.4	100 mM K^+	1.1×10^{-7}	0.55
	8.0	–	1.0×10^{-7}	0.61
Pur2-Cross	5.0	–	5.3×10^{-8}	1.2
	7.2	–	8.0×10^{-8}	0.76
	7.4	100 mM K^+	6.1×10^{-8}	1.0
	8.0	–	7.0×10^{-8}	0.87
Pur2-Modified Cross	8.0	–	9.9×10^{-8}	0.62

[a]Values of K_d were calculated from equation **2** as described in Materials and Methods.
[b]Relative affinity = $K_{d,ref}/K_d$, where $K_{d,ref}$ indicates the affinity of **Pur2-Cross** binding at pH 7.4 in the presence of 100 mM K^+.

Oligonucleotide binding affinities

Equilibrium dissociation constants (K_ds) were measured for triplexes in the *bcl-2* promoter at various pH values in the range 5.0–8.0. Typically, pyrimidine motif triplexes require cytidine protonation and are stabilized by acidic pH, while the stabilities of purine motif triplexes are thought to be intrinsically pH independent. Figure 2A and B presents examples of binding experiments at pH

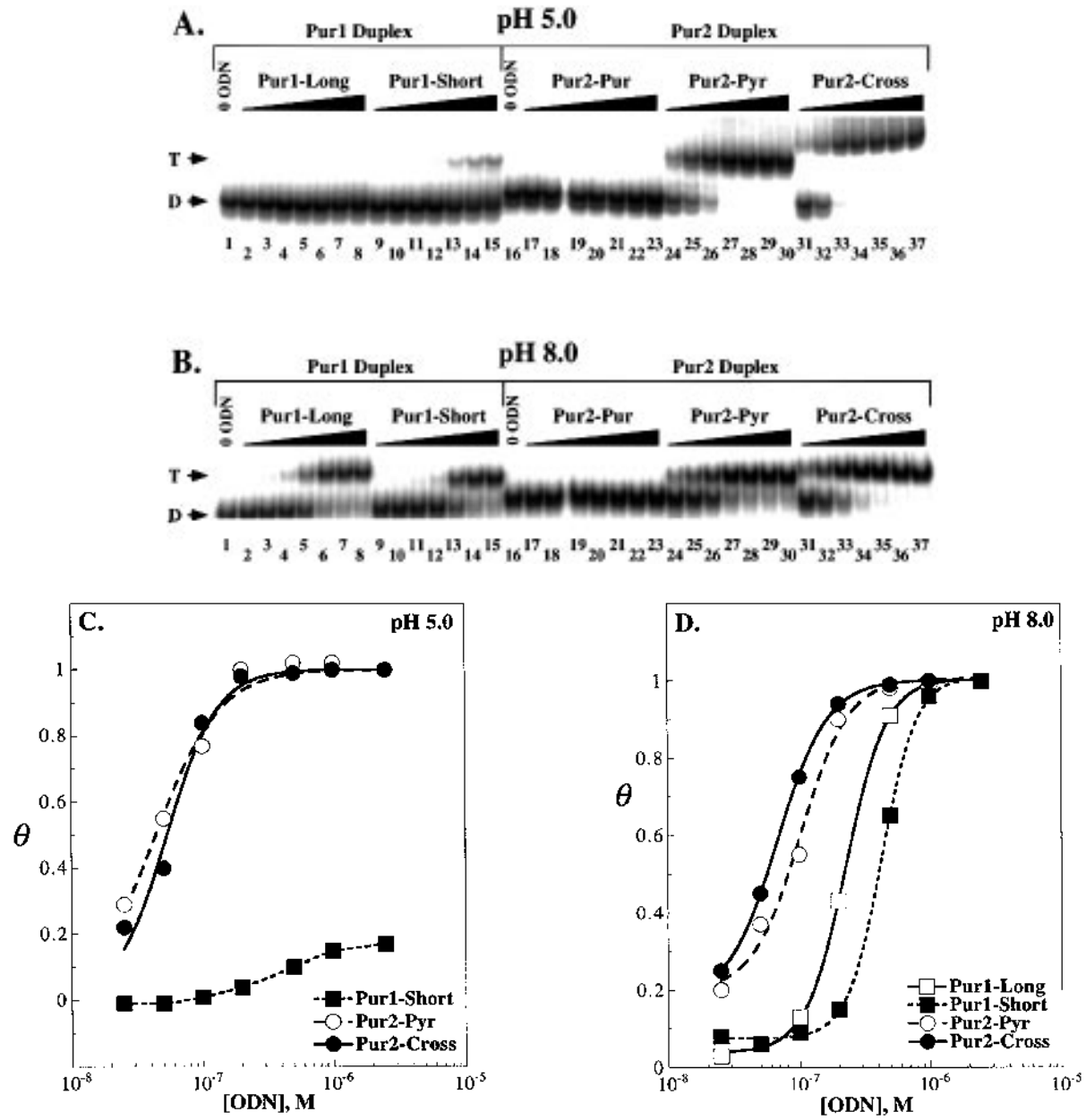

Figure 2. Determination of triplex K_d. (**A** and **B**) Electrophoretic mobility shift assays at pH 5.0 (A) or pH 8.0 (B). Increasing micromolar concentrations (0.025, 0.05, 0.1, 0.2, 0.5, 1, 2.5) of **Pur1-Long** (lanes 2–8), **Pur1-Short** (lanes 9–15), **Pur2-Pur** (lanes 17–23), **Pur2-Pyr** (lanes 24–30), **Pur2-Cross** (lanes 31–37) or no oligonucleotide (lanes 1 and 16) were added to labeled target Pur1 duplex (lanes 1–15) or Pur2 duplex (lanes 16–37). Mobilities of free duplex (D) and triplex (T) are indicated. (**C** and **D**) Binding curves for **Pur1-Long** (□), **Pur1-Short** (■), **Pur2-Pyr** (○) and **Pur2-Cross** (●) with respective target duplex were fitted using data from electrophoretic mobility shift titrations at pH 5.0 (C) or pH 8.0 (D). The fraction of duplex in triplex form (θ) was calculated from equation **1** and fitted to equation **2** as described in Materials and Methods to provide estimates of K_d (Table 1).

5.0 and 8.0 respectively, in which labeled Pur1 and Pur2 duplexes were incubated in the presence of increasing oligonucleotide concentrations. Figure 2C and D depicts quantitative results from these experiments. Values of K_d were calculated as described in Materials and Methods and are listed in Table 1. At pH 5.0, purine motif oligonucleotides **Pur1-Long** and **Pur1-Short** bound the Pur1 duplex target weakly with K_d values >>2.5×10^{-6} M (Fig. 2A and C). As the pH was increased, oligonucleotide binding in the purine motif increased, with K_d values of 2.3×10^{-7} M and 4.7×10^{-7} M for **Pur1-Long** and **Pur1-Short** respectively, at pH 8.0 (Fig. 2B and D). This result contradicts the conventional view that triple helix formation in the purine motif is pH independent. However, the basis for suppression of purine motif triplexes at low pH remains unclear.

Purine motif oligonucleotide **Pur2-Pur** did not detectably bind the Pur2 duplex under any pH condition tested, perhaps due to its short length. Both **Pur2-Pyr** and **Pur2-Cross** bound the Pur2 duplex with high affinity at pH 5.0 (K_d values of 4.4×10^{-8} M and 5.3×10^{-8} M respectively; Fig. 2A and C). Surprisingly, the affinities of these oligonucleotides decreased only slightly at higher pH values (K_d values of 1.0×10^{-7} M and 7.0×10^{-8} M for **Pur2-Pyr** and **Pur2-Cross** respectively at pH 8.0; Fig. 2B and D). The impressive

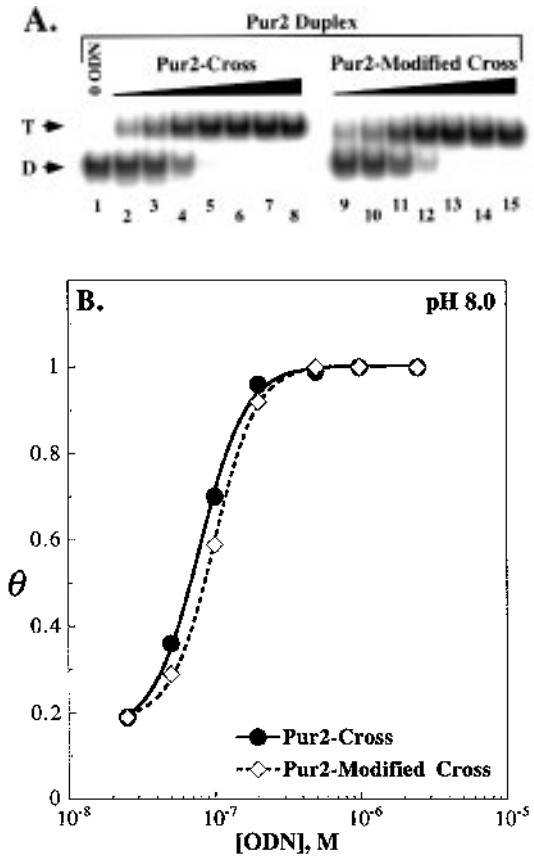

Figure 3. K_d comparison of **Pur2-Cross** with **Pur2-Modified Cross**. (**A**) Electrophoretic mobility shift assay. Increasing micromolar concentrations (0.025, 0.05, 0.1, 0.2, 0.5, 1, 2.5) of **Pur2-Cross** (lanes 2–8), **Pur2-Modified Cross** (lanes 9–15) or no oligonucleotide (lane 1) were added to labeled target Pur2 duplex. Mobilities of free duplex (D) and triplex (T) are indicated. (**B**) Binding curves for **Pur2-Cross** (●) and **Pur2-Modified Cross** (◇) with Pur-2 duplex were fitted using data from electrophoretic mobility shift titrations. The fraction of duplex in triplex form (θ) was calculated from equation **1** and fitted to equation **2** as described in Materials and Methods to provide estimates of K_d (Table 1).

ability of these oligonucleotides to bind with high affinity at pH values ≤8.0 emphasizes the sequence-dependence of triplex affinity. Particularly favorable features of these oligonucleotides may be their thymidine-richness, and absence of the requirement to protonate any consecutive cytidine residues. Binding affinities of **Pur2-Pyr** and **Pur2-Cross** were also tested in the presence of a pseudo-physiological pH 7.4 buffer containing 100 mM K^+ (intracellular $[K^+]$ is thought to be ~100–200 mM; 33). The observed binding affinity for **Pur2-Cross** ($K_d = 6.1 \times 10^{-8}$ M) was nearly 2-fold higher than for **Pur2-Pyr** ($K_d = 1.1 \times 10^{-7}$ M). The Pur2 sequence therefore provides an example of a duplex target where alternate-strand triple helix formation increases oligonucleotide binding affinity under pseudo-physiological conditions, relative to the binding of oligonucleotides to either individual domain.

It is interesting to note that triplexes containing **Pur2-Cross** have a slightly lower electrophoretic mobility at pH 5.0 than at 8.0 (compare lanes 31–37 of Fig. 2A and B). This decrease in mobility at low pH may indicate a less compact structure consistent with partial release of the purine motif portion of the complex (31). This result is in accord with the observation that purine motif triplexes involving **Pur1-Long** and **Pur1-Short** are unstable at pH 5.0 (Fig. 2A).

If high affinity triplex binding to the promoter region of *bcl-2* were considered for the therapeutic enhancement of apoptosis, it would presumably be beneficial to reduce degradation by nucleases. We wished to study whether modifications previously shown to confer nuclease resistance might be tolerated in the *bcl-2* triplexes. Because **Pur2-Cross** had the highest affinity of any oligonucleotide studied under pseudo-physiological conditions, we used its sequence to design nuclease-resistant **Pur2-Modified Cross** (Fig. 1B). The purine motif portion of the sequence was modified using a nuclease-resistant phosphorothioate backbone (34). However, such modifications are not permissive for triplex formation in the pyrimidine motif (35). Therefore, the pyrimidine motif portion of **Pur2-Modified Cross** was made nuclease-resistant by substituting 2′-*O*-methylthymidine for all thymidines (36). Stabilities of triplexes involving **Pur2-Cross** versus **Pur2-Modified Cross** were determined by incubation of the labeled Pur2 duplex with increasing oligonucleotide concentrations at pH 8.0 (Fig. 3A and B). The K_d value of **Pur2-Modified Cross** (9.9×10^{-8} M) was not substantially lower than that of **Pur2-Cross** (7.0×10^{-8} M).

Details of oligonucleotide specificity and duplex structure

To verify specificity and monitor any changes in target structure upon oligonucleotide binding to the Pur1 and Pur2 duplexes, a DMS footprinting analysis was performed. Protection of guanine N7 from DMS modification is conferred by triple helix formation. After cloning into plasmids, targeted guanines in the Pur1 sequence were specifically, (though weakly) protected by 1 μM of both **Pur1-Long** and **Pur1-Short** in pH 8.0 binding buffer (Fig. 4A, lanes 3 and 4 respectively). Although this weak footprint indicates a relatively low binding affinity, the high level of background cleavage of this sequence (Fig. 4A, lane 1) should also be noted. The slight hypermethylation of guanines just 3′ of the **Pur1-Short** binding domain is a phenomenon often seen at sequences adjacent to triplex binding sites and may reflect structural changes in the duplex at the duplex–triplex junction.

In contrast with results at the Pur1 site, guanines within the 21 base homopurine domain on the bottom strand of the Pur2 duplex are strongly protected by **Pur2-Pyr**, **Pur2-Cross** and **Pur2-Modified Cross** under pseudo-physiological conditions (Fig. 4A, lanes 7, 8 and 9). Again, significant hypermethylation of the 3′-most guanine of the target sequence is observed in the presence of **Pur2-Pyr**. Hypermethylation of this guanine is increased further when the target sequence is bound by **Pur2-Cross** and **Pur2-Modified Cross** (Fig. 4B). Note that in an attempt to optimize traversal of the major groove to the alternate strand, these oligonucleotides have been designed with deletion of the cytidine residue that would normally bind this 3′ guanine. Some characteristic of the oligonucleotide transition between alternate strands may increase the perturbation of the duplex structure at this sequence.

As evidence of the simultaneous recognition of alternate DNA strands, it is noteworthy that guanines within the nine base homopurine domain on the top strand of the Pur2 duplex are also strongly protected by **Pur2-Cross** and **Pur2-Modified Cross** under pseudo-physiological conditions (Fig. 4A, lanes 14 and 15). The 3′-most guanine in this domain is also hypermethylated in the presence of **Pur2-Cross** and **Pur2-Modified Cross**, most likely due to duplex structural changes at this junction (Fig. 4B).

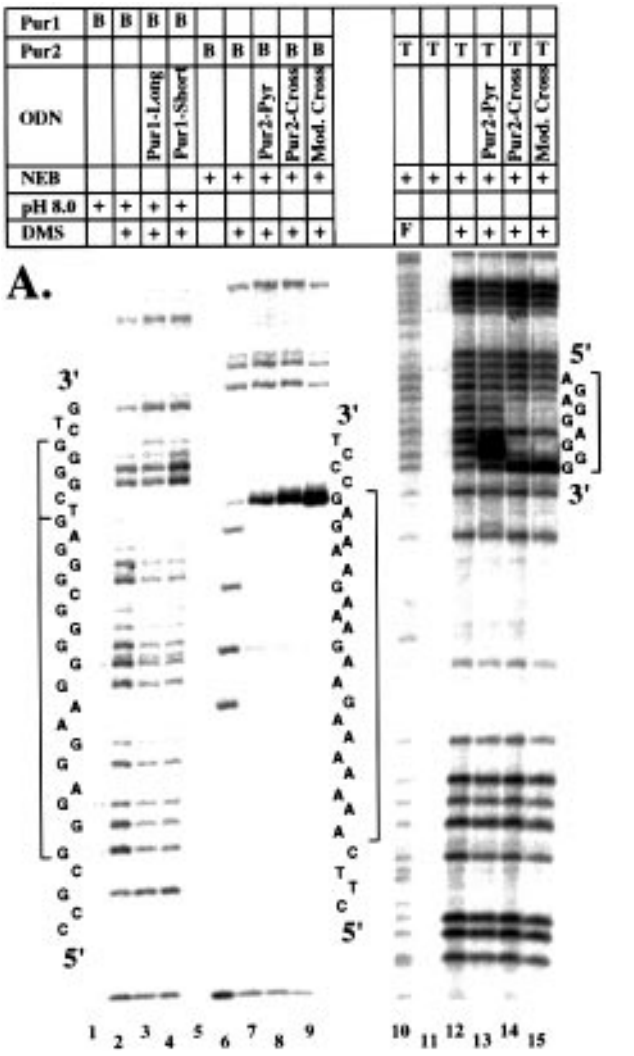

Figure 4. Dimethyl sulfate footprinting assay. (**A**) The Pur1 and Pur2 duplexes were subcloned into a recombinant plasmid that was then linearized, labeled on the top or bottom strand, and subjected to DMS modification in the absence or presence of 1 μM oligonucleotide (ODN) and the indicated binding buffer [pH 8.0 or nuclear extraction buffer (NEB)] as described in Materials and Methods. The target sites for triplex formation are bracketed and their polarities labeled. B, bottom strand labeling; T, top strand labeling; F, formic acid treatment to generate an A+G ladder. (**B**) Recognition of Pur2 duplex by **Pur2-Cross**, which crosses the major groove to bind alternate strand homopurine domains. Potential triplet hydrogen bonds are denoted by dots. Guanines that are hypermethylated by DMS when the Pur2 duplex is bound by either **Pur2-Cross** or **Pur2-Modified Cross** are boxed. Guanines that are circled indicated hypermethylation by DMS when the Pur2 duplex is bound by **Pur2-Pyr**.

Methylation can be detected at the 3′ intervening adenine within the target sequence, and this adenine remains unprotected in the presence of either **Pur2-Cross** or **Pur2-Modified Cross**. As expected, protection of this domain is not observed in the presence of **Pur2-Pyr**, which binds only to the alternate strand (Fig. 4A, lane 13). However, this oligonucleotide does induce hypermethylation of two guanines within the homopurine region of this strand, again suggesting structural changes induced by triplex formation (Fig. 4B). These data confirm oligonucleotide specificities and provide strong evidence for the ability of **Pur2-Cross** and **Pur2-Modified Cross** to simultaneously bind to alternate DNA strands.

DISCUSSION

We have used the purine and pyrimidine triple helix motifs to design several oligonucleotides to recognize two target sequences in the *bcl-2* P1 promoter. At physiological pH, oligonucleotides **Pur2-Pyr** and **Pur2-Cross** bound the Pur2 target sequence with K_d values near 1×10^{-7} M, affinities ~10-fold higher than observed for oligonucleotides **Pur1-Long** and **Pur1-Short** binding to the Pur1 target sequence. **Pur2-Cross**, designed to bind alternate strand homopurine domains, had the highest affinity of all oligonucleotides tested under pseudo-physiological conditions ($K_d = 6.1 \times 10^{-8}$ M).

In the course of binding studies under various pH conditions, we were surprised that purine motif oligonucleotides **Pur1-Long** and **Pur1-Short** bound the Pur1 duplex very weakly at low pH. Although there is no intrinsic pH requirement for reverse Hoogsteen hydrogen bonding in the purine motif, this study clearly demonstrates a strong pH dependence for triplexes at this sequence. Triplexes involving **Pur1-Long** and **Pur1-Short** were also seen to be inhibited by physiological levels of monovalent cations, particularly K^+ (data not shown). This is in agreement with previous studies that demonstrate purine motif triplex inhibition by monovalent cations (37–39). Such inhibition is most likely caused by competing equilibria wherein the guanine-rich oligonucleotides become sequestered into guanine quartet aggregates (39). Incorporation of 6-thioguanine into a limited number of positions of purine motif oligonucleotides has been shown to alleviate ion inhibition of triplexes (40,41) and could potentially be used as a strategy to permit **Pur1-Long** and **Pur1-Short** to form triplexes under pseudo-physiological conditions.

In contrast with the purine motif oligonucleotides, pyrimidine motif oligonucleotides **Pur2-Pyr** and **Pur2-Cross** not only tolerated physiological ion concentrations, but were remarkably pH independent, being stable at pH 8.0. This result is notable in light of the requirement for cytidine protonation in the pyrimidine motif. The presence of 5-methylcytidine (Me^5C) in **Pur2-Pyr** and **Pur2-Cross** is likely to be a large contributor to this pH independence. Previous studies have indicated that Me^5C substitution allows certain oligonucleotide sequences to form triplexes at pH values >7, though the mechanism of stabilization is unclear (32). However, the pH independence of **Pur2-Pyr** and **Pur2-Cross** is also sequence dependent, as triplexes involving other pyrimidine motif oligonucleotides containing Me^5C are destabilized at neutral pH (data not shown). Perhaps thymidine-rich sequences lacking consecutive cytidines are most favorable for triplex stability >pH 7. Together with the results of previous studies (3–5,8), these data reinforce the view that conventional purine motif triplexes are stabilized by profoundly guanine-rich target strands, while conventional pyrimidine motif triplexes are stabilized by adenine-rich target strands punctuated with isolated guanine residues.

Another key result from these studies is the high affinity binding of alternate strand homopurine domains in the *bcl-2* promoter by **Pur2-Cross**. In particular, **Pur2-Cross** recognizes the nine base homopurine domain of the Pur2 duplex to which oligonucleotide

Pur2-Pur could not detectably bind. Moreover, the simultaneous recognition of both homopurine domains of the Pur2 duplex increases the affinity of **Pur2-Cross** almost 2-fold relative to the affinity of **Pur2-Pyr** under pseudo-physiological conditions. These results support previous studies in which alternate strand triple helix formation was shown to allow binding of adjacent homopurine domains of <10 bases when oligonucleotides could not bind either domain individually (27). In addition, the present study provides evidence that alternate strand binding can increase the stability of a triple helix relative to binding a single domain of >10 bases. A previous study of alternate strand binding to domains >10 bases demonstrated a modest 1.4-fold increase in affinity relative to binding a single domain (31).

DMS hypermethylation of guanines adjacent to duplex–triplex junctions is a common observation that presumably reflects perturbations in the duplex structure upon oligonucleotide binding (31,42). An alternative hypothesis to explain the observed hypermethylation is that the terminal unstacked bases at triplex/duplex junctions creates a hydrophobic microenvironment that increases the local DMS concentration. Binding of **Pur1-Short** and **Pur2-Pyr** to target duplexes in this study promoted hypermethylation of the purine strand 3′ to the complex. In the case of **Pur2-Pyr**, hypermethylation of a pair of guanines was also seen on the opposite DNA strand at the same end of the complex. Interestingly, binding of **Pur2-Cross** caused an increase in hypermethylation at junction guanines on both strands of the target duplex. This suggests a strain or distortion in the duplex when **Pur2-Cross** traverses the major groove between alternate strands, thus causing the major groove to be more accessible to DMS. Such a distortion could reflect an energy expense associated with alternate strand binding (31). Optimized oligonucleotide designs might reduce this apparent distortion.

Together, the results of this study indicate that a natural sequence in the human *bcl-2* promoter can form a stable triplex with a synthetic oligonucleotide under pseudo-physiological conditions. Moreover, it is promising that this oligonucleotide can be modified to increase nuclease resistance without a significant decrease in binding affinity. Extension of these studies to intact cells will require attention to several obstacles: oligonucleotide delivery to the nucleus, availability of DNA target sites within chromatin structure, and the unknown effects of these triplex complexes on *bcl-2* transcription. *In vitro* studies have shown that occlusion of transcription factor binding sites by triplexes can block transcription initiation (11,43,44). Other studies indicate that direct overlap of protein and triplex binding sites may not be necessary for transcriptional inactivation by triplexes (2,11,13). The latter results suggest that oligonucleotide binding may alter duplex DNA structure in some manner (bending, stiffening) so as to antagonize promoter function (11). It is provocative to note that both Pur1 and Pur2 target sequences are located on or near consensus Sp1 binding sites within the P1 *bcl-2* promoter. Further studies will be necessary to determine if triple-helical complexes identified in the present study will offer a feasible approach to transcriptional inhibition of the *bcl-2* gene in living cells.

ACKNOWLEDGEMENTS

We gratefully acknowledge D. Eicher and C. Mountjoy for their excellent technical assistance. This work was supported by NIH grant GM 47814 and a Junior Faculty Research Award from The American Cancer Society to L.J.M. W.M.O. is supported by a University of Nebraska Medical Center Presidential Fellowship.

REFERENCES

1 Moser, H. E. and Dervan, P. B. (1987) *Science*, **238**, 645–650.
2 Cooney, M., Czernuszewicz, G., Postel, E. H., Flint, S. J. and Hogan, M. E. (1988) *Science*, **241**, 456–459.
3 Hélène, C. (1991) *Anti-Cancer Drug Design*, **6**, 569–584.
4 Maher, L. J. (1992) *BioEssays*, **14**, 807–815.
5 Maher, L. J., III. (1996) *Cancer Invest.*, **14**, 66–82.
6 Maher, L. J., Wold, B. and Dervan, P. B. (1989) *Science*, **245**, 725–730.
7 Maher, L. J., Dervan, P. B. and Wold, B. J. (1990) *Biochemistry*, **29**, 8820–8826.
8 Maher, L. J., III, Dervan, P. B. and Wold, B. (1991) In Wickstrom, E. (ed.) *Prospects for Antisense Nucleic Acid Therapy of Cancer and AIDS*. Wiley-Liss, New York, pp. 227–242.
9 Orson, F. M., Thomas, D. W., McShan, W. M., Kessler, D. J. and Hogan, M. E. (1991) *Nucleic Acids Res.*, **19**, 3435–3441.
10 Young, S. L., Krawczyk, S. H., Matteucci, M. D. and Toole, J. J. (1991) *Proc. Natl Acad. Sci. USA*, **88**, 10023–10026.
11 Maher, L. J., Dervan, P. B. and Wold, B. (1992) *Biochemistry*, **31**, 70–81.
12 Maher, L. J. (1992) *Biochemistry*, **31**, 7587–7594.
13 Duval-Valentin, G., Thuong, N. T. and Hélène, C. (1992) *Proc. Natl Acad. Sci. USA*, **89**, 504–508.
14 Beal, P. A. and Dervan, P. B. (1991) *Science*, **251**, 1360–1363.
15 Hockenbery, D. M. (1995) *BioEssays*, **17**, 631–638.
16 Steller, H. (1995) *Science*, **267**, 1445–1449.
17 Thompson, C. B. (1995) *Science*, **267**, 1456–1462.
18 White, E. (1993) *Genes Dev.*, **7**, 2277–2284.
19 Williams, G. T. and Smith, C. A. (1993) *Cell*, **74**, 777–779.
20 Vaux, D. L., Weissman, I. L. and Kim, S. K. (1992) *Science*, **258**, 1955–1957.
21 Oltvai, Z. N., Milliman, C. L. and Korsmeyer, S. J. (1993) *Cell*, **74**, 609–619.
22 Katsumata, M., Siegel, R. M., Louie, D. C., Miyashita, T., Tsujimoto, Y., Nowell, P. C., Greene, M. I. and Reed, J. C. (1992) *Proc. Natl Acad. Sci. USA*, **89**, 11376–11380.
23 Seto, M., Jaeger, U., Hockett, R. D., Graninger, W., Bennett, S., Goldman, P. and Korsmeyer, S. J. (1988) *EMBO J.*, **7**, 123–131.
24 Veis, D., Sorenson, C., Shutter, J. and Korsmeyer, S. J. (1993) *Science*, **75**, 229–240.
25 Cantor, C. R. and Schimmel, P. R. (1980) *Biophysical Chemistry, Part I: The Conformation of Biological Macromolecules.*, Freeman, San Francisco, p. 864.
26 Young, R. L. and Korsmeyer, S. J. (1993) *Mol. Cell. Biol.*, **13**, 3686–3697.
27 Beal, P. A. and Dervan, P. B. (1992) *J. Am. Chem. Soc.*, **114**, 4976–4982.
28 Jayasena, S. D. and Johnston, B. H. (1992) *Biochemistry*, **31**, 320–327.
29 Jayasena, S. D. and Johnston, B. H. (1992) *Nucleic Acids Res.*, **20**, 5279–5288.
30 Jayasena, S. D. and Johnston, B. H. (1993) *Biochemistry*, **32**, 2800–2807.
31 Olivas, W. M. and Maher, L. J., III. (1994) *Biochemistry*, **33**, 983–991.
32 Povsic, T. J. and Dervan, P. B. (1989) *J. Am. Chem. Soc.*, **111**, 3059–3061.
33 Alberts, B., Bray, D., Lewis, J., Raff, M., Roberts, K. and Watson, J. D. (1983) *Molecular Biology of the Cell*, Garland Publishing, Inc., New York, p. 286.
34 Stein, C. A. and Cheng, Y.-C. (1993) *Science*, **261**, 1004–1012.
35 Hacia, J. G., Wold, B. J. and Dervan, P. B. (1994) *Biochemistry*, **33**, 5367–5369.
36 Sproat, B. S., Lamond, A. I., Beijer, B., Neuner, P. and Ryder, U. (1989) *Nucleic Acids Res.*, **17**, 3373–3386.
37 Milligan, J. F., Krawczyk, S. H., Wadwani, S. and Matteucci, M. D. (1993) *Nucleic Acids Res.*, **21**, 327–333.
38 Cheng, A.-J. and Van Dyke, M. W. (1993) *Nucleic Acids Res.*, **21**, 5630–5635.
39 Olivas, W. M. and Maher, L. J., III. (1995) *Biochemistry*, **34**, 278–284.
40 Rao, T. S., Durland, R. H., Seth, D. M., Myrick, M. A., Bodepudi, V. and Revankar, G. R. (1995) *Biochemistry*, **34**, 765–772.
41 Olivas, W. M. and Maher, L. J., III. (1995) *Nucleic Acids Res.*, **23**, 1936–1941.
42 Collier, D. A., Mergny, J.-L., Thuong, N. T. and Hélène, C. (1991) *Nucleic Acids Res.*, **19**, 4219–4224.
43 Grigoriev, M., Praseuth, D., Robin, P., Hemar, Saison-Behmoaras, T., Dautry-Versat, A., Thuong, N.T., Hélène, C. and Harel-Bellan, A. (1992) *J. Biol. Chem.*, **267**, 3389–3395.
44 Grigoriev, M., Praseuth, D., Guieysse, A., Robin, P., Thuong, N. and Hélène, C. (1993) *Proc. Natl Acad. Sci. USA*, **90**, 3501–3505.